Design of an Underwater Acoustic MIMO OFDM System Using NI LabVIEW and CompactDAQ

Peng Chen
School EECMS
Curtin University
Bentley, WA, Australia
y.rong@curtin.edu.au

Yue Rong
School EECMS
Curtin University
Bentley, WA, Australia
y.rong@curtin.edu.au

Sven Nordholm
School EECMS
Curtin University
Bentley, WA, Australia
s.nordholm@curtin.edu.au

Alec Duncan
CMST
Curtin University
Bentley, WA, Australia
a.j.duncan@curtin.edu.au

Zhiqiang He
Key Lab UWC
BUPT
Beijing, China
hezq@bupt.edu.cn

***Abstract*—Recently, the orthogonal frequency-division multiplexing (OFDM) technology is receiving increasing attention in underwater acoustic (UA) communications. This paper presents the design of a real-time UA OFDM communication system with multiple transducers and hydrophones using the National Instruments CompactDAQ device and LabVIEW software. The purpose of this system is to provide academic researchers a flexible and reconfigurable multiple-input multiple-output (MIMO) UA communication transceiver with an open-architecture to conveniently test and validate the performance of their MIMO transceiver algorithms, which is missing in the literature. The system design, including both the transmitter and receiver, is discussed. The performance of this MIMO UA communication system is verified through a UA communication experiment conducted in the Canning River, Western Australia. Compared with existing modems, the proposed implementation simplifies the prototype design and supports MIMO functions.**

***Index Terms*—Underwater acoustic communication, OFDM, Multiple hydrophones, LabVIEW**

I. Introduction

The underwater acoustic (UA) channel is one of the most challenging channels for wireless communication, due to its extremely limited bandwidth, strong multipath interference, and significant Doppler shifts [1]. Recently, orthogonal frequency-division multiplexing (OFDM) systems have been proposed for UA communication because of their ability to mitigate rapid frequency dispersion with a reasonable computational complexity [2]-[6].

In [5], an implementation of OFDM-based modems for UA communication using the TMS320C6713 digital signal processor (DSP) development board has been demonstrated. A comprehensive literature survey of software-defined UA modems is provided in [7]. It is worth noting that DSP-based implementations can be time-consuming on system hardware and software design and implementation, particularly for UA communication systems with multiple transducers and hydrophones.

In this paper, an National Instruments (NI) LabVIEW-based implementation of a real-time UA OFDM transceiver prototype with multiple transducers and hydrophones is proposed. It is important to note that our prototype is not aiming at increasing the data rate and/or the range of UA communication, which is the goal of most commercial UA modems. Indeed, the purpose of the proposed system is to provide academic researchers a flexible and reconfigurable multiple-input multiple-output (MIMO) UA communication transceiver with an open-architecture to conveniently test and validate the performance of their MIMO transceiver algorithms.

There are many software-defined UA modems with very good performance for their applications [7], for example, the GNU radio based systems [8], [9] and LabVIEW-based UA prototypes [10], [11]. However, based on our best knowledge, our implementation is the first one which is based on LabVIEW and supports MIMO OFDM functions.

Both the transmitter and receiver system designs are discussed in this paper. The performance of this system is verified through a UA communication experiment conducted in the Canning River, Western Australia. Experimental results show that the system achieves a reliable bit-error-rate (BER) performance. In particular, for a single transducer system, the system BER can be significantly reduced by equipping the receiver with two hydrophones compared with a single hydrophone. Moreover, the system data rate can be greatly increased by installing multiple transducers at the transmitter. Compared with [11], which focuses on a UA communication system with a single transducer and a single hydrophone, this paper provides more details on the design and performance analysis of UA OFDM communication systems with multiple transducers and hydrophones.

The remainder of this paper is organized as follows. The model of a UA OFDM system with multiple transducers and hydrophones is presented in Section II. The system software implementation is presented in Section III. The results of the river experiments are demonstrated in Section IV. In Section V, conclusions are drawn.

II. System Model

In this paper, we use LabVIEW to implement a frame-based coded MIMO UA OFDM communication system. The block diagram of the proposed transmitter system is illustrated in Fig. 1. In each frame, a binary source data stream of L_b bits is encoded to form a sequence of L_c bits. The coded sequence is mapped into data symbols drawn from the phase-shift keying (PSK) or quadrature amplitude modulation (QAM) constellations. Then every N_s data symbols together with N_p quadrature PSK (QPSK) modulated pilot symbols are mapped

Global Oceans 2020: Singapore - U.S. Gulf Coast | 978-1-7281-5446-6/20/$31.00 ©2020 IEEE | DOI: 10.1109/IEEECONF38699.2020.9389319

978-1-7281-5446-6/20/$31.00 ©2020 IEEE

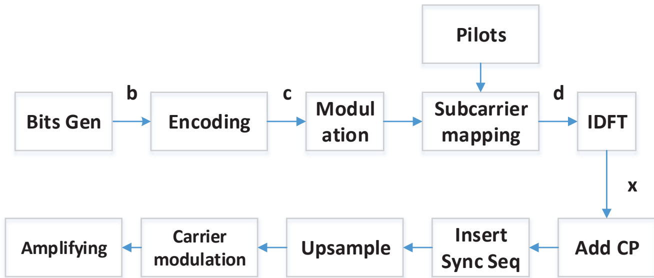

Fig. 1. Block diagram of the transmitter in a UA OFDM communication system.

into an $N_c \times 1$ OFDM symbol vector $\boldsymbol{d}_t$ at the t-th transducer, $t = 1, \ldots, N_t$, where N_c is the total number of subcarriers and N_t is the number of transducers. The pilot subcarriers are uniformly spaced. Each OFDM symbol is converted to the time domain by the inverse discrete Fourier transform (IDFT), and a cyclic prefix (CP) with length T_{cp} longer than the channel delay spread is then prepended to the time domain symbol.

At the receiver end, after downshifting, low-pass filtering, and removing the CP, the baseband discrete time samples of one OFDM symbol at the r-th hydrophone can be written as

$$\boldsymbol{y}_r = \sum_{t=1}^{N_t} \boldsymbol{P}_{r,t}\boldsymbol{F}^H\boldsymbol{D}_t\boldsymbol{h}_{r,t} + \boldsymbol{w}_r, \quad r = 1, \ldots, N_r$$

where $\boldsymbol{F}$ is an $N_c \times N_c$ DFT matrix with the (i,k)-th entry of $1/\sqrt{N_c}e^{-j2\pi(i-1)(k-1)/N_c}$, $i,k = 1, \ldots, N_c$, $(\cdot)^H$ denotes the matrix Hermitian transpose, $\boldsymbol{D}_t = \mathrm{diag}(\boldsymbol{d}_t)$ is a diagonal matrix taking $\boldsymbol{d}_t$ as the main diagonal elements, $\boldsymbol{h}_{r,t}$ is the channel frequency response between the t-th transducer and the r-th hydrophone, $\boldsymbol{w}_r$ is the additive noise vector, $\boldsymbol{P}_{r,t} = \mathrm{diag}(\boldsymbol{p}_{r,t})$, $\boldsymbol{p}_{r,t} = (1, e^{-j2\pi f_{r,t}/B}, \ldots, e^{-j2\pi(N_c-1)f_{r,t}/B})^T$ is the phase distortion caused by the Doppler shift, $(\cdot)^T$ denotes the vector transpose, B is the bandwidth of the transmitted signal, and $f_{r,t}$ is the frequency offset of the channel between the t-th transducer and the r-th hydrophone. In this paper, we assume that all channels experience a similar Doppler frequency offset.

III. System Design

The key parameters of the UA OFDM system are summarized in Table I. A list of system hardware and their functions in the UA MIMO OFDM system is shown in Table II. The software of our UA communication system is designed and implemented using NI LabVIEW. In the following, we present the system software design at the transmitter and the receiver.

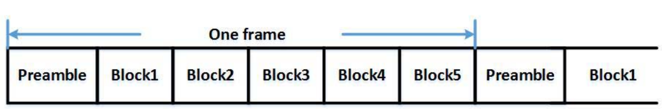

Fig. 2. Frame structure of the transmitted signals.

TABLE I
UA OFDM System Parameters

Carrier frequency	f_c	12 kHz
Sampling rate	R_s	48 kHz
Bandwidth	B	4 kHz
Number of subcarriers	N_c	512
Subcarrier spacing	f_{sc}	7.8 Hz
Length of OFDM symbol	T	128 ms
Length of CP	T_{cp}	25 ms

TABLE II
A List of System Hardware

Device Name	Device Function
NI cDAQ-9174	Transfer data between computer and I/O devices
NI-9232	Acquire signals from the hydrophones
NI-9260	Output signals to the transducers
CTG0052	Transmitter transducers
HTI-96-Min	Receiver hydrophones

1) Transmitter: The system we designed occupies the frequency band from 10 kHz to 14 kHz with a bandwidth of $B = 4$ kHz. The sampling rate is 48 kHz. Note that the system software can be easily modified to cater for transducers working at other frequency bands. Fig. 2 illustrates the data frame structure of the transmitted signals. We can see from Fig. 2 that each frame contains $N_b = 5$ OFDM data blocks and one preamble block. In each data block, there are $N_c = 512$ subcarriers and $T_{cp} = 25$ ms. The preamble block, which consists of a $N_{pn} = 127$-pseudo noise sequence followed by N_{pn} zeros, is used for synchronization and frame head detection. Among the 512 subcarriers, there are 325 data subcarriers, 128 uniformly spaced pilot subcarriers and 59 null subcarriers for frequency offset estimation. The data symbols are modulated by either QPSK or 16-QAM constellations encoded by 1/3 rate turbo codes. In each data frame, the number of information-carrying bits is $L_b = 1088N_t$ for the QPSK modulation and $L_b = 2176N_t$ for the 16-QAM modulation scheme. The system source data rate is

$$R_b = \frac{N_t L_b}{(N_c/B+T_{cp})N_b + 2N_{pn}/B} = \begin{cases} 1.31N_t \text{ kb/s}, & \text{QPSK} \\ 2.63N_t \text{ kb/s}, & \text{16-QAM} \end{cases}.$$

It can be seen that the source data rate increases with the number of transducers and the modulation size.

2) Receiver: The baseband signal processing at the receiver is shown in Fig. 3. It can be seen that for signals received at each hydrophone, the receiver performs frequency offset estimation and compensation for each OFDM symbol using the null subcarriers, and then the baseband signals are passed through channel estimation. The channel estimator uses the least-squares method to estimate the frequency domain channel response at the pilot subcarriers. Note that to avoid interference, the pilot sequences from all N_t transducers are orthogonal to each other. The linear interpolation algorithm is then adopted by the estimator to estimate the data subcarrier channel response based on pilot subcarrier channel responses. Channel equalization is performed on the received signals

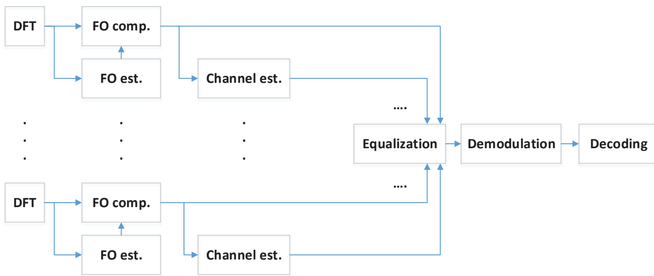

Fig. 3. Block diagram of the baseband signal processing at the receiver.

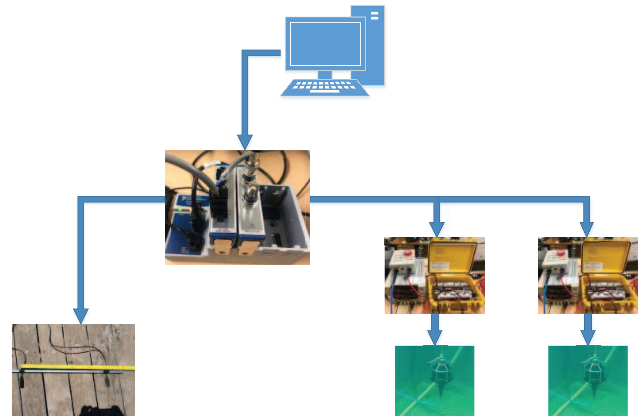

Fig. 4. Experimental system setup.

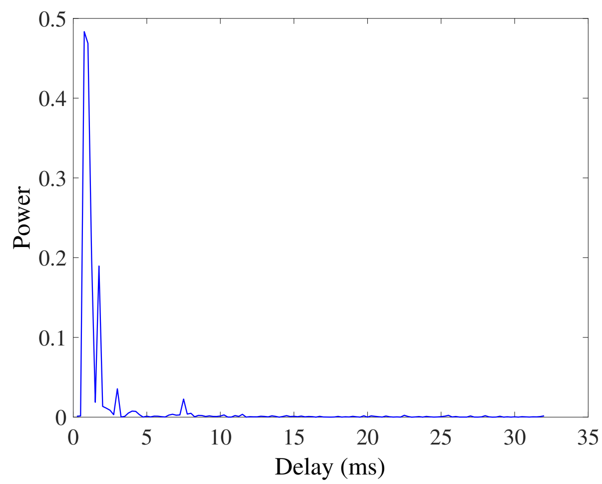

Fig. 5. Channel impulse response estimated by the pilot subcarriers.

using the estimated channel response. In particular, in the single transducer mode, the maximum ratio combining technique is used to combine signals from multiple hydrophones. In the MIMO mode, the zero-forcing algorithm is adopted to equalize signals received from the hydrophones. Demodulation is performed on the equalized data subcarriers leading to a raw bit sequence. The raw bit sequence is finally passed through a turbo decoder. Note that compared with systems with a single transducer and hydrophone [9]-[11], the receiver design of a MIMO UA communication system is more complicated. In order to reduce the system computation time, the turbo encoder and decoder are implemented in the C language and embedded into the system via the dynamic-link library technology.

IV. Experiment Results

In this section, we study the performance of our LabVIEW-based real-time MIMO UA OFDM system. The experimental system setup is shown in Fig. 4. In particular, the NI cDAQ-9174 chassis is connected to a desktop computer through a USB cable where the NI LabVIEW software is installed for signal generation and processing. The NI-9232 and NI-9260 modules are plugged into slot 1 and slot 2 of the cDAQ-9174 chassis, respectively. Two CTG0052 transducers each with a power amplifier and matching network are connected to channel 0 and channel 1, respectively, of the NI-9260 module for transmitting acoustic signals. Channel 1 and 2 of NI-9232 are connected to two HTI-96-Min hydrophones through preamplifiers for the acquisition of the real-time acoustic signals. During the experiment, the amplitude of the transmitted signals is controlled through a parameter α, which in turn determines the signal-to-noise ratio at the receiver.

A. Single Transducer Multi-hydrophone Experiment

A UA communication experiment using the system we developed was conducted in the Canning River, Western Australia. Canning River has brackish water with varying salinity. In this experiment, only one transducer was used for transmitting signals, and was attached through a cable and located about half a meter above the river bed. Two hydrophones at the receiver were also located around half a meter above the river bed. The distance between the hydrophones and the transducer was around 10 m and the water depth was approximately 1.5 m.

A typical channel impulse response between one transducer and one hydrophone during the experiment estimated by the pilot subcarriers is shown in Fig. 5. It can be seen that the maximal channel delay spread is around 10 ms which is shorter than the length of the CP. This verifies that the system parameters are correctly chosen.

During the experiment, we set α to 6.3×10^{-4}, 7.1×10^{-4}, 7.9×10^{-4}, 8.9×10^{-4}, 1×10^{-3}, and 1.4×10^{-3}, respectively. This is approximately equal to a change in the transmission power of 1 dB between two adjacent transmissions except for the last one which is around a 3 dB change. Fig. 6 illustrates the BER performance of the proposed system with the 16-QAM modulation scheme. It can be seen that the system BER performance is significantly improved by combining the signals received from two hydrophones. In particular, using two hydrophones brings about 2 dB and 4 dB power gain over the first channel and the second channel, respectively. It can also be observed from Fig. 6 that the BER performance of the second channel is worse than that of the first channel. The reason for this is that during the experiment, we observed that the second hydrophone suffers from a higher background

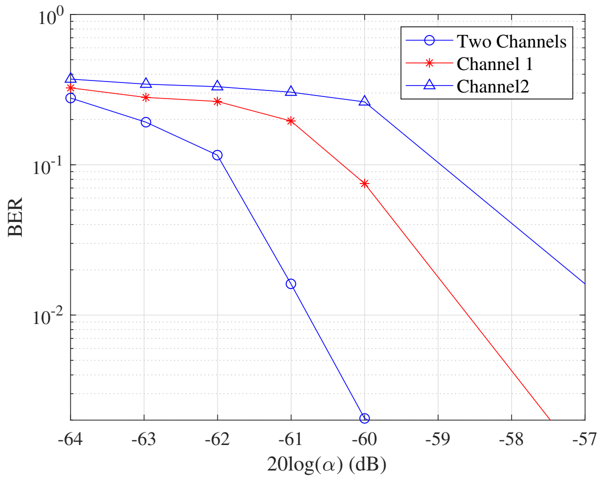

Fig. 6. BER of the system with one transducer and two hydrophones.

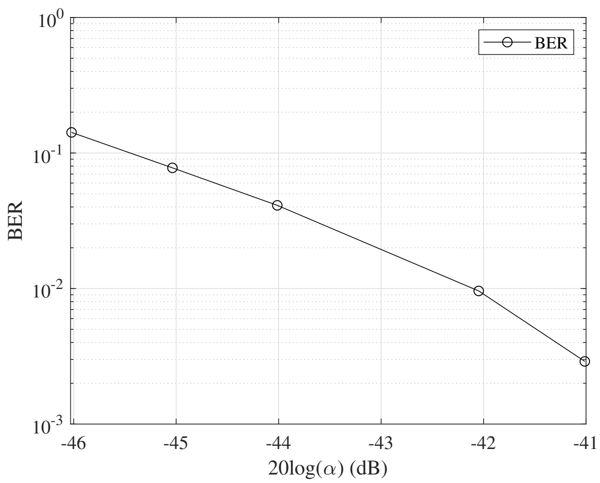

Fig. 7. BER of the system with two transducers and two hydrophones.

noise level than the first hydrophone.

B. Multi-Transducer Multi-hydrophone Experiment

Another UA communication experiment using the system shown in Fig. 4 was conducted in the Canning River, Western Australia. Two hydrophones and two transducers were used in this experiment to verify the performance of a MIMO system. The two transducers were located about 0.2 m above the river bed and the distance between them was 0.75 m. The two hydrophones were located around 0.5 m above the river bed and were attached to a steel bar with a distance of 0.5 m between them. The distance between the transducers and hydrophones was around 10 m.

To evaluate the BER performance of the MIMO system, we varied the transmission power through adjusting the amplification factor α for the two transducers. Note that the two transducers always use the same α. We set α to 5×10^{-3}, 5.6×10^{-3}, 6.3×10^{-3}, 7.9×10^{-3}, and 8.9×10^{-3}, respectively. This is approximately equivalent to changing the transmission power by 1 dB or 2 dB between two adjacent transmissions. The system BER with the 16-QAM modulation scheme versus α is shown in Fig. 7. By comparing Fig. 7 with Fig. 6, it can be seen that the MIMO system has a higher BER. The reasons are twofold. Firstly, two data streams are transmitted concurrently in the MIMO system, while only a single data stream is transmitted in the single transducer multi-hydrophone system. Thus, the latter system has a higher order of spatial diversity, leading to a lower BER. However, the MIMO system has doubled the data rate of the latter system. Such rate-BER tradeoff needs to be considered in the design of practical UA OFDM systems. Secondly, we observed that during the MIMO experiment, there was much more impulsive noise at the receiver hydrophones from waves breaking at the jetty piers due to strong wind.

V. Conclusions

In this paper, an NI CompactDAQ and LabVIEW-based implementation of real-time UA OFDM system with multiple hydrophones and transducers has been presented. This system provides academic researchers a flexible and reconfigurable MIMO UA communication transceiver with an open-architecture to conveniently test and validate the performance of their MIMO algorithms. River tests have been conducted to verify the performance of the system developed.

References

[1] D. Kilfoyle and A. Baggeroer, "The state of the art in underwater acoustic telemetry," *IEEE J. Ocean. Eng.*, vol. 25, no. 1, pp. 4-27, Jan. 2000.

[2] M. Chitre, S. H. Ong, and J. Potter, "Performance of coded OFDM in very shallow water channels and snapping shrimp noise," in *Proc. MTS/IEEE OCEANS*, Washington, DC, Sep. 2005, pp. 996–1001.

[3] P. Chen, Y. Rong, S. Nordholm, Z. He, and A. Duncan, "Joint channel estimation and impulsive noise mitigation in underwater acoustic OFDM communication systems," *IEEE Trans. Wireless Commun.*, vol. 16, no. 9, pp. 6165-6178, Sep. 2017.

[4] P. Chen, Y. Rong, S. Nordholm, and Z. He, "Joint channel and impulsive noise estimation in underwater acoustic OFDM systems," *IEEE Trans. Veh. Technol.*, vol. 66, no. 11, pp. 10567-10571, Nov. 2017.

[5] H. Yan, L. Wan, S. Zhou, Z. Shi, J. H. Cui, J. Huang, and H. Zhou, "DSP based receiver implementation for OFDM acoustic modems," *Phys. Commun.*, vol. 5, no. 1, pp. 22-32, 2012.

[6] S. Wang, Z. He, K. Niu, P. Chen, and Y. Rong, "New results on joint channel and impulsive noise estimation and tracking in underwater acoustic OFDM systems," *IEEE Trans. Wireless Commun.*, vol. 19, no. 4, pp. 2601-2612, Apr. 2020.

[7] H. S. Dol, P. Casari, T. van der Zwan, and R. Otnes, "Software-defined underwater acoustic modems: Historical review and the NILUS approach," *IEEE J. Ocean. Eng.*, vol. 42, no. 3, pp. 722-737, Jul. 2017.

[8] E. Demirors, G. Sklivanitis, T. Melodia, S. N. Batalama, and D. A. Pados, "Software-defined underwater acoustic networks: Toward a high-rate real-time reconfigurable modem," *IEEE Commun. Magazine*, vol. 53, no. 11, pp. 64-71, Nov. 2015.

[9] E. Demirors, G. Sklivanitis, G. E. Santagati, T. Melodia, and S. N. Batalama, "A high-rate software-defined underwater acoustic modem with real-time adaptation capabilities," *IEEE Access*, vol. 6, pp. 18602-18615, 2018.

[10] L. E. Emokpae, S. E. Freeman, G. F. Edelmann, and D. M. Fromm, "Highly directional multipath free high data-rate communications with a reconfigurable modem," *IEEE J. Ocean. Eng.*, vol. 44, no. 1, pp. 229-239, Jan. 2019.

[11] P. Chen, Y. Rong, S. Nordholm, and Z. He, "An underwater acoustic OFDM system based on NI CompactDAQ and LabVIEW," *IEEE Systems Journal*, vol. 13, no. 4, pp. 3858-3868, Dec. 2019.